Journal of Applied Fluid Mechanics, Vol. 5, No. 3, pp. 79-87, 2012.
Available online at www.jafmonline.net, ISSN 1735-3572, EISSN 1735-3645.
DOI: 10.36884/jafm.5.03.19448

Effect of Axial Conduction and Variable Properties on Two-Dimensional Conjugate Heat Transfer of Al_2O_3-EG/Water Mixture Nanofluid in Microchannel

A. Ramiar and A.A. Ranjbar [1†] and S.F. Hosseinizadeh

[1]*Professor, Babol University of Technology, Babol, Iran, P.O. Box 484*

†*Corresponding Author Email: ranjbar@nit.ac.ir*

(Received July 22, 2010; accepted June 1, 2011)

ABSTRACT

Conjugate heat transfer of a nanofluid containing Al_2O_3 nanoparticles dispersed in a mixture of 60% ethylene glycol and 40% water by mass (60:40 EG/W) in a two dimensional microchannel has been solved numerically. The effect of axial conduction in both solid and liquid regions has been considered in a range of Reynolds numbers in laminar regime. The utilized nanofluid models are capable of considering variation of thermal conductivity and dynamic viscosity with temperature. The results show that using nanoparticles with higher thermal conductivities will enhance heat transfer characteristics of the channel. Comparing the nanofluid with pure mixture revealed that adding nanoparticles will decrease conduction number which is a scale of axial conduction. Also, it was found that considering variable properties will cause severe changes to the Nusselt number distribution especially for low Reynolds numbers.

Keywords: Conjugate heat transfer, Nanofluid, Graetz number, Conduction number, Microchannel

NOMENCLATURE

b	thickness ratio, H_s/H
Cp	Constant pressure specific heat, J/kgK
Gz	Graetz number, Re Pr D_h/x
H	Height of the channel
Nu	Nusselt number, hd/k
P	Pressure, N/m^2
Pr	Prandtl number
q_w	heat transfer rate at the wall, W/m^2
Re	Reynolds number
T	Temperature, K
T_b	Bulk temperature, K
U	velocity, m/s

Greek Symbols

φ	Volume fraction of nanoparticles
μ	Dynamic viscosity, Pa.s
ρ	Density, kg/m^3

Superscripts

Ave	Average at the inlet
f	Fluid
nf	nanofluid
p	nanoparticles
s	solid

1. INTRODUCTION

The compactness and high surface-to-volume ratios of microscale liquid flow devices make them attractive alternatives to conventional flow systems for heat transfer augmentation, chemical reactor or combustor miniaturization and aerospace technology implementations.

Tuckerman and Pease (1981), were first to introduce the concept of microchannel heat sinks for high heat flux removal and employ water flowing under laminar conditions in silicon microchannels. Afterwards, various aspects of the fluid flow in microchannel have been studied experimentally and numerically. Some of them, such as Li *et al.* (2007), Hetsroni *et al.* (2005) and Lee and Garimella (2006) have done experimental observations to analyze microchannels from friction and heat transfer point of view and others such as Gamrat *et al.* (209) and Xie *et al.* (2009) studied numerical aspects of them.

Nanofluids have been proposed as a mean to enhance the performance of heat transfer liquids currently available. Recent experiments on nanofluids have indicated significant increase in thermal conductivity compared with liquids without nanoparticles or larger particles, strong temperature dependence of thermal

conductivity and significant increases in critical heat flux in boiling heat transfer. Fluid flow and heat transfer of nanofluid in different geometries have been studied by several authors such as Santra *et al.* (2009) and Nonino *et al.* (2009) but there are little works related to the nanofluid flow in microchannel. Koo and Kleinstreuer (2005) studied the effect of nanoparticles concentrations on different parameters of microchannel heat sinks. They considered two combinations of copper oxide nanoparticles in water or ethylene glycol and used their own models for the effective thermal conductivity and dynamic viscosity for nanofluids. Their results proved the ability of nanofluids to enhance the performance of heat sinks.

Jang and Choi (2006) used their thermal conductivity model (Jang and Choi (2004)) to predict thermal performance of microchannel heat sinks using nanofluids. Their results showed an enhancement of 10% for water-based nanofluids containing diamond (1 vol.%, 2 nm) at the fixed pumping power. Tsai and Chein (2007) addressed analytically the effect of adding copper nanoparticle and carbon nanotube to water in performance of Microchannel heat sink. It was found that using nanofluid can enhance the Microchannel heat sink performance when the porosity and aspect ratio are less than the optimum porosity and aspect ratio and for higher porosity and channel aspect ratio than this value the enhancement of using nanofluid is not significant. Bhattacharya *et al.* (2009) analyzed numerically laminar forced convective conjugate heat transfer characteristics of Al_2O_3/H_2O nanofluid flowing in a silicon microchannel heat sink. They found that the improvement of microchannel heat sink performance due to use of nanofluid becomes more pronounced with increase in nanoparticle concentration. They also showed that fully developed heat transfer coefficient for nanofluid flow in microchannel heat sink increases with Reynolds number even in laminar flow regime rather than a constant. Ho *et al.* (2010) investigated enhancement of forced convective heat transfer in a copper microchannel heat sink with Al_2O_3-water nanofluid of 1 and 2 vol.% as the coolant and the Reynolds number ranging from 226 to 1676. It was demonstrated that adding nanofluids significantly increase the average heat transfer coefficient.

In this paper, the effect of concentration of Al_2O_3 nanoparticles in 60:40 EG/Water mixture will be studied from hydrodynamic and heat transfer point of view. Then, the effect of solid region type on axial conduction and also the effect of variable properties on thermal performance of the fluid will be considered.

2. MATHEMATICAL MODEL

2.1 Geometry

Steady, forced laminar convection flow and heat transfer of a nanofluid flowing inside a straight 2D microchannel will be solved. The geometry of the 2D Microchannel is shown in Fig. 1. The channel height is H= 80 μm and its length is L= 10 cm. Al_2O_3-60:40 EG/Water nanofluid enters the channel in a constant temperature of 298 K and constant velocity. The solid region is made of silicon (k_s=120 W/mK) with different heights from b= H_s/H=1 to 100.

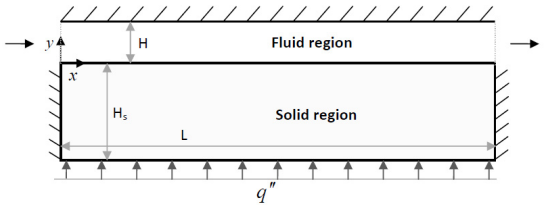

Fig. 1. The geometry of the 2D microchannel

The effect of changing the thermal conductivity of the solid region will be studied in this paper, by considering different values of k_s.

2.2 Governing Equations

Xuan and Roetzel (2000) suggested that by considering thermal equilibrium between nanoparticles and the base fluid and neglecting the velocity slip, one can simplify the nanofluid as a single fluid with modified properties. Comparing the results of using this assumption with experimental observations showed good agreement between them. Utilizing the aforementioned assumptions, for the steady flow and heat transfer of an incompressible nanofluid in a 2D, the Continuity, momentum and energy equations are:

$$\nabla.\vec{u} = 0 \tag{1}$$

$$(\vec{u}.\nabla)\vec{u} = -\frac{1}{\rho_{nf}}\nabla p + \frac{1}{\rho_{nf}}\nabla.(\mu_{nf}\nabla\vec{u}) \tag{2}$$

$$(\vec{u}.\nabla)T = \frac{1}{(\rho c_p)_{nf}}\nabla.(k_{nf}\nabla T) \tag{3}$$

And the energy equation for the solid region is:

$$k_s\nabla^2 T = 0 \tag{4}$$

2.2 Boundary Conditions

Boundary conditions for the fluid region are:

No-slip condition for all solid surfaces, or u=v=0 at y=0 and y=H, uniform velocity and temperature distribution profile at the inlet:

$$u = u_{in}, T = T_{in} \qquad 0 \le y \le H \tag{5}$$

At the outlet, zero normal stress and outflow condition for temperature field are considered:

$$\frac{\partial u}{\partial x} = 0, \frac{\partial T}{\partial x} = 0 \qquad 0 \le y \le H \tag{6}$$

A uniform heat flux is imposed from the down wall of solid region:

$$-K_s\frac{\partial T_s}{\partial y} = q'' \qquad y = -H_s \tag{7}$$

and at the interface of the solid and liquid region, conjugate heat transfer boundary condition is implied:

$$K_s\left(\frac{\partial T_s}{\partial y}\right)_{solid} = K_{nf}\left(\frac{\partial T_f}{\partial y}\right)_{nanofluid} \tag{8}$$

$$, (T_s)_{solid} = (T_f)_{nanofluid} \qquad y = 0$$

All other walls are adiabatic:

$$\frac{\partial T_s}{\partial x} = 0 \qquad x = 0,\ x = L \tag{9}$$

$$\frac{\partial T_f}{\partial x} = 0 \qquad y = H \tag{10}$$

2.3 Nanofluid Properties

Considering the nanofluid as a single phase fluid, properties of the mixture (nanofluid) as a function of concentration of nanoparticles can be determined as follows:

Density and heat capacitance of the nanofluid are simply determined from:

$$(\rho)_{nf} = (1-\varphi)\rho_f + \varphi\rho_p \tag{11}$$

$$(\rho c_p)_{nf} = (1-\varphi)(\rho c_p)_f + \varphi(\rho c_p)_p \tag{12}$$

where φ is the particle volume fraction and subscripts f, nf and p stand for base fluid, nanofluid and nanoparticles, respectively. The well known model of Hamilton and Crosser (1962) for the thermal conductivity of the nanofluid which is based on Maxwell's theory is:

$$\frac{k_{nf}}{k_f} = \frac{k_p + (n-1)k_f + (n-1)(k_p - k_f)\varphi}{k_p + (n-1)k_f - (k_p - k_f)\varphi} \tag{13}$$

Where k_p and k_f are thermal conductivities of nanoparticles and base fluid, and n is the empirical shape factor (=3 for spherical nanoparticles). Besides this model and other simple models, some models for thermal conductivity have been recently proposed which considers parameters such as temperature, Brownian motion and sublayer thickness.

Chon *et al.* (2005) introduced a model which has been used and suggested for CuO and Al_2O_3-water nanofluids (Mintsa *et al.* 2009):

$$\frac{k_{nf}}{k_f} = 1 + 64.7\varphi^{0.746}\left(\frac{d_f}{d_p}\right)^{0.369}\left(\frac{k_p}{k_f}\right)^{0.7476} \mathrm{Pr}^{0.9955}\,\mathrm{Re}^{1.2321} \tag{14}$$

d_f and d_p are diameter of the molecule of the base fluid and nanoparticles respectively.

$\mathrm{Pr} = \dfrac{\mu_f}{\rho_f \alpha_f}$ and $\mathrm{Re} = \dfrac{\rho_f k_b T}{3\pi\mu^2 l_f}$ are specific Prandtle number and Reynolds number, respectively where α_f is the thermal diffusivity, k_b is the Boltzmann constant and l_f is the mean free path of the base fluid which has been considered equal to 0.17 nm for water.

There are a vast range of different relations for calculating the dynamic viscosity of nanofluid. Value of this property has a substantial effect on hydrodynamic and heat transfer characteristics of nanofluid. Many of the literature suggest using the well known relation of Brinkman (1952) for dynamic viscosity:

$$\frac{\mu_{nf}}{\mu_f} = \frac{1}{(1+\varphi)^{2.5}} \tag{15}$$

It is claimed by several authors that this relation is proper for concentration less than 5%. Maiga *et al.* (2004) suggested the relation for dynamic viscosity based on experimental data of Wang *et al.* (1999). For Al_2O_3- water nanofluid they proposed:

$$\frac{\mu_{nf}}{\mu_f} = 123\varphi^2 + 7.3\varphi + 1 \tag{16}$$

Masoumi *et al.* (2009) developed a new model for dynamic viscosity which considers Brownian motion, temperature and diameter of nanoparticles:

$$\frac{\mu_{nf}}{\mu_f} = 1 + \frac{\rho_p V_B d_p^2}{72 N \delta} \tag{17}$$

where $\delta = \sqrt[3]{\dfrac{\pi}{6\varphi}}\, d_p$ is the distance between centers of the particles, $V_b = \dfrac{1}{d_p}\sqrt{\dfrac{18 k_b T}{\pi\rho_p d_p}}$ is the Brownian velocity. $N = (c_1\varphi + c_2)\, d_p + (c_3\varphi + c_4)$ is the fitting parameter which its constants has been determined by fitting with experimental results. Suggested values for these constant parameters are: $c_1 = -1.133e^{-6}$, $c_2 = -2.771e^{-6}$, $c_3 = 9.0e^{-8}$ and $c_1 = -3.93e^{-7}$.

Some of the aforementioned relations are general and can be applied to any combination of fluids and particles but are not much exact, such as Eq. (13) and Eq. (15), but some others such as Eq. (14) are specially obtained for limited combinations and lead to rather exact results. There are scarce relations specially for nanofluids containing nanoparticles of Al_2O_3 or CuO in mixture of 60% ethylene glycol and 40% water (60:40 EG/W). Recently vajjha and coworkers have done some experiments with this combination of nanofluids and developed new correlations to compute different properties.

Vajjha and Das (2009) developed a new correlation for calculating thermal conductivity of Al_2O_3 and CuO nanoparticles dispersed in a 60:40 EG/W mixture. Their model is based on the model of Koo and Kleinstreuer (2004), which is a combination of the static part of Maxwell's theory (Eq. 13) and a dynamic part considering the Brownian motion of nanoparticles.

$$k_{nf} = \frac{k_p + 2k_f + 2(k_p - k_f)\varphi}{k_p + 2k_f - (k_p - k_f)\varphi} k_f + 5\times10^4\, \beta\varphi\rho_f C_{p_f} \sqrt{\frac{k_b T}{\rho_p d_p}} f(T,\varphi) \tag{18}$$

They obtained the f function from their experimental results as:

$$f(T,\varphi) = \left(2.8217\times10^{-2}\varphi + 3.917\times10^{-3}\right)\frac{T}{T_0} - \left(3.0669\times10^{-2}\varphi + 3.91123\times10^{-3}\right) \tag{19}$$

T_0 is a reference temperature which is equal to 293. β is $8.4407\times(100\varphi)^{-1.07307}$ for Al_2O_3 nanoparticles and $9.881\times(100\varphi)^{-0.9446}$ for CuO nanoparticles in the range of $0<\varphi<0.1$. Vajjha (2009) introduced a relation for dynamic viscosity of Al_2O_3 and CuO nanoparticles dispersed in 60:40 EG/W mixture:

$$\frac{\mu_{nf}}{\mu_f} = A\,e^{B\varphi} \tag{20}$$

Where μ_f is the dynamic viscosity of the mixture and can be obtained from available references, for example the curve fitted relation derived by the author from data of ASHRAE (2005) is:

$$\mu_f = C\,e^{\frac{D}{T}} \tag{21}$$

The constants in the above equations are:

$$C = 0.555\times10^{-3},\ D = 2664 \text{ for } 293K < T < 363 \tag{22}$$

For Al_2O_3 nanoparticles in 60:40 EG/W mixture:

$$A = 0.983,\ B = 12.959 \text{ for } 293K < T < 363 \tag{23}$$

and for CuO nanoparticles in 60:40 EG/W mixture:

$$A = 0.9197,\ B = 22.8539 \text{ for } 293K < T < 363 \tag{24}$$

Here we use Eq. (18) for thermal conductivity and Eq. (20) for dynamic viscosity of the nanofluid.

3. Numerical Computation

The finite volume method is used to solve governing equations in a collocated grid arrangement and the well-known Rhie and Chow (see Ferziger and Peric (2002)) interpolation scheme is used for pressure-velocity coupling. In order to achieve more precise results a third order QUICKER scheme of Pollard and Siu (1982) is used to descritize the governing equations.

3.1 Grid Sensivity

The entire computational domain is discretized using different grid arrangements of 500×5 (for fluid region) and 500×10 (for solid region), 1000×10 and 1000×20, 1500×15 and 1500×30, 2000×20 and 2000×40, 2500×25 and 2500×50. The fluid is 60:40 EG/Water mixture without nanoparticles and $\mathrm{Re}_f = \frac{\rho_f u_{ave} H}{\mu_f} = 500.$

u_{ave} is the average velocity of the fluid or uniform inlet velocity. As it is shown in Fig. 2, comparing the results for different grids yield the selection of 2000×20 mesh for the fluid region and 2000×40 mesh for the solid region as a satisfactory grid-independence arrangement.

3.2 Validation of the Code

The fluid flow with Pr=0.7 in a channel without solid region is considered for validation of the results by comparing with the formula presented by Bejan and Sciubba (1992) for Nusselt number distribution along the channel.

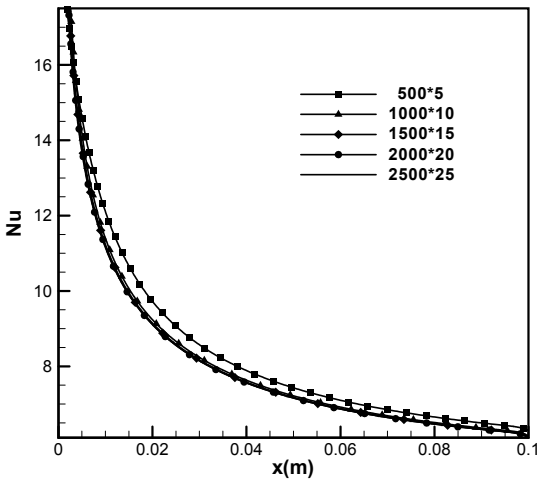

Fig. 2. Grid independent study

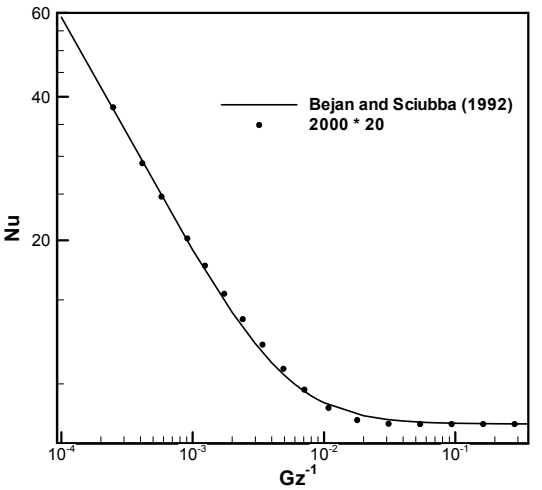

Fig. 3. Validation of the code

Figure 3 shows the validation study conducted for the microchannel (L = 0.07 m, H = 500 μm), at Re = 800. A 2000×20 mesh is appropriate for the problem considered and the results are in good agreement with the experimental fitted formula.

4. Numerical Results

The effect of nanoparticles' concentration on enhancement of the heat transfer in microchannel is depicted in Fig. 4. The variation of Nusselt number in the down wall of the channel are shown in this figure for Re_f=150, b=7 and different volume fractions. The Nusselt number in a 2D channel flow is defined as:

$$Nu = \frac{k_{nf}}{k_f}\frac{2}{(T_w - T_b)}\left.\frac{\partial T}{\partial y}\right|_{wall} \tag{25}$$

where T_w is the temperature of the wall and the bulk temperature is defined by:

$$T_b = \frac{\int_0^H u\,T\,dy}{\int_0^H u\,dy} \tag{26}$$

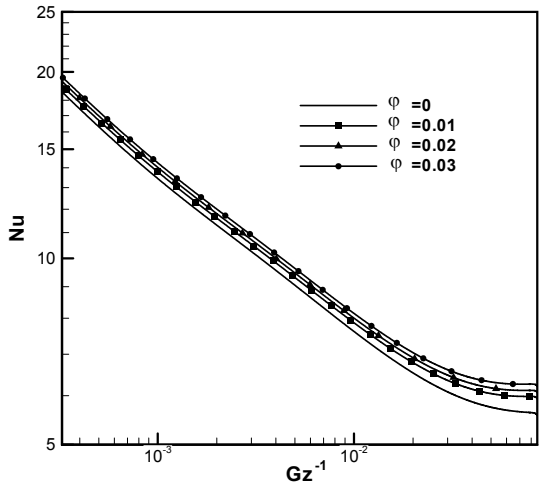

Fig. 4. Distribution of lower wall Nusselt number in horizontal direction for Re_f=150, b=7 and q_w=10^5 w/m^2.

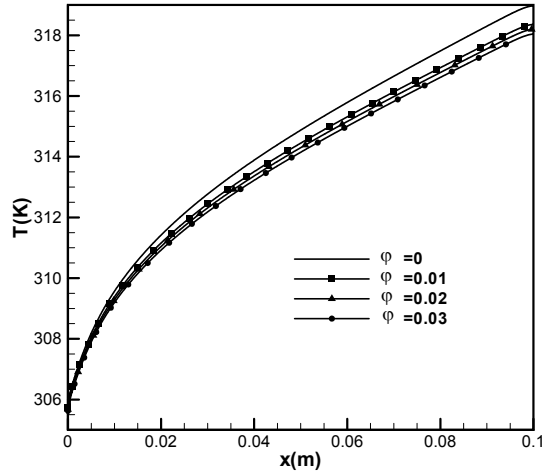

Fig. 5. Distribution of lower wall temperature in horizontal direction for Re_f=150, b=7 and q_w=10^5 w/m^2.

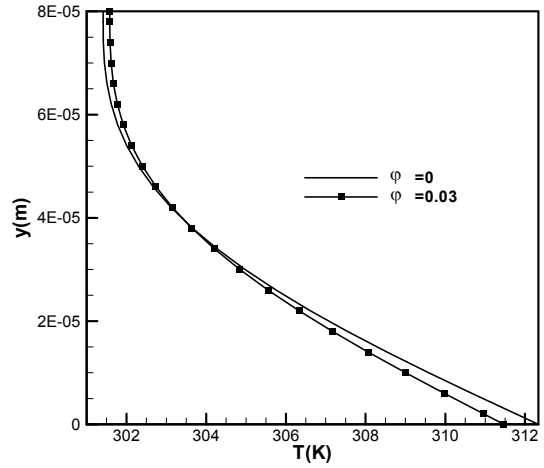

Fig. 6. Temperature profiles at the middle of the channel (Re_f=150, b=7 and q_w=10^5 w/m^2).

Adding nanoparticles will increase the local Nusselt number and enhance thermal characteristics of the fluid. The fully developed Nusselt number of EG/Water-Al_2O_3 nanofluid with φ = 0.03 is approximately 11.2% higher than that of pure EG/Water mixture. This enhancement is a good achievement for nanofluids to be used in heat exchangers as a means of intensification of heat transfer process.

As a result of the presence of nanoparticles, the fluid can remove more heat from the solid surface and lessens the temperature of the fluid-solid interface. This means that more heat can be removed by the nanofluid. This effect is illustrated in Fig. 5 for an imposed constant heat flux of q_w=10^5 W/m^2.

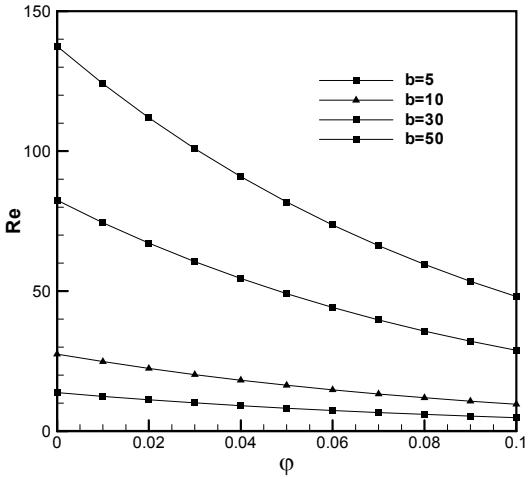

Fig. 7. Critical Reynolds numbers for various values of height ratio of the channel

Another aspect of improvement, caused by nanofluids is depicted in Fig. 6. The figure shows the temperature profile at the middle of the channel for the case described at previous figure. Nanoparticles will help the fluid to diffuse heat and this phenomenon called "dispersion" can be seen in this figure as a tendency of temperature profile of the fluid to be flattened by increasing the volume fraction of the nanoparticles.

4.1 Effect of Axial Conduction

Chiou (1980) introduced the Conduction number (C) to describe the effect of the axial heat conduction in the wall on convection heat transfer quantitatively:

$$C = \frac{Conduction\ \ in\ \ wall}{Convection\ \ in\ \ fluid} = \frac{k_s}{k_f}\frac{A_s}{A_f}\frac{D_h}{L}\frac{1}{\mathrm{Re\,Pr}} \tag{27}$$

where *s* and *f* subscripts stand for solid and fluid regions. He suggested that the effect of axial heat conduction in the channel wall on the convective heat transfer can be ignored, if the Conduction number is less than 0.005. Here we use a critical Conduction number of 0.02 which is suggested by Morini (2006). For the 2D microchannel considered here:

$$C = \frac{k_s}{k_f}\frac{H_s}{H}\frac{2H}{L}\frac{1}{\mathrm{Re\,Pr}} \tag{28}$$

Using the corresponding values of the problem, we can find a critical Reynolds number value for each b=H_s/H below which the conjugate effects cannot be neglected. Figure 7 shows the critical Reynolds numbers for different volume fractions of the Al_2O_3-EG/Water nanofluid in a channel with different height ratios. As seen, adding nanoparticles will decrease the critical

Reynolds number, it means that axial conduction should be considered in lower Reynolds numbers than that of pure fluid. The changes seem considerable in higher height ratios and for b=50 the critical Reynolds number changes from Re ≈ 137 in φ =0 to Re ≈ 48 in φ = 0.1 but this effect is not considerable for lower height ratios.

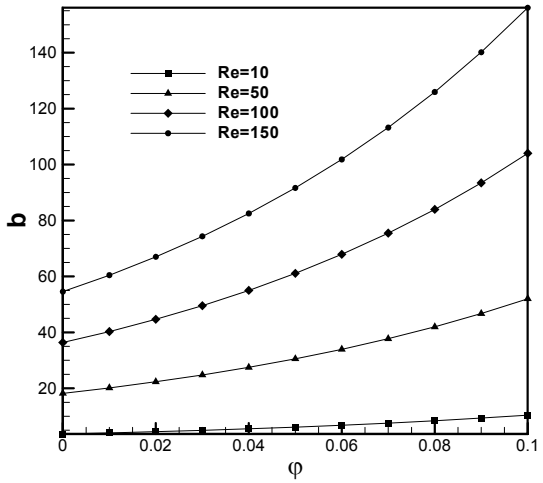

Fig. 8. Critical height ratios of the channel for various Reynolds numbers

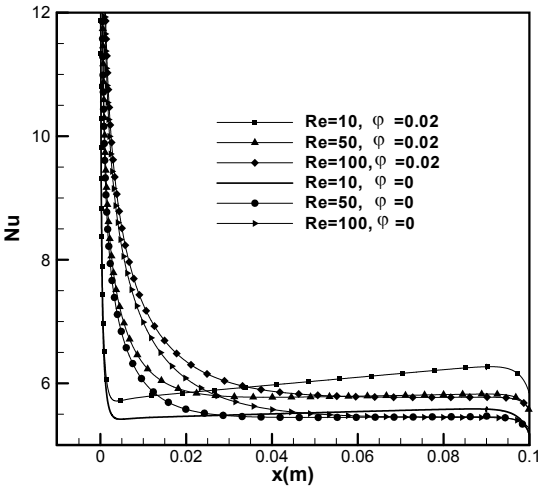

Fig. 9. Nanofluid concentration effect on Nusselt number distribution for different Reynolds numbers

On the other hand, one can find a critical height ratio for each Reynolds number above which the conjugate effect should be considered. As seen in Fig. 8, in Re=100, the critical height ratio varies from b ≈ 36 in φ =0 to b ≈ 104 in φ = 0.1. We can conclude from Figs. 7 and 8 that adding nanoparticles will weaken the conjugate effect and for example in the case of Re=100, the solid region must be thicker (b>36) to affect the temperature distribution in fluid region.

Effect of axial conduction on Nusselt number distribution can be demonstrated by reducing the Reynolds number to values less than critical one. Figure 9 depicts the variation of Nusselt number in horizontal direction for 0 and 2% volume fractions of Al_2O_3-EG/Water nanofluid flowing in a b=7 channel and Reynolds number changing from 100 to 10. In higher Reynolds numbers, the entrance length, increases and this will cause an enhancement in heat transfer. In higher Reynolds numbers, the fully developed Nusselt number for each volume fraction converges to the same value, but in lower Reynolds numbers, axial conduction in the channel will affect the Nusselt number in entrance region and a sudden decrease will happen. This will cause a reduction in average Nusselt number. This phenomenon has been reported by other researchers such as Nonino *et al.* (2009). On the other hand, such minima also appear in some of the local Nusselt number axial distributions obtained numerically by Lelea (2007) and experimentally by Lelea *et al.* (2004).

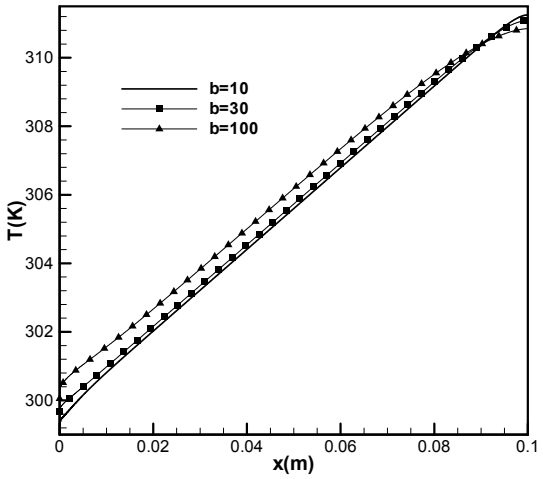

Fig. 10. The effect of solid region height on the lower wall temperature

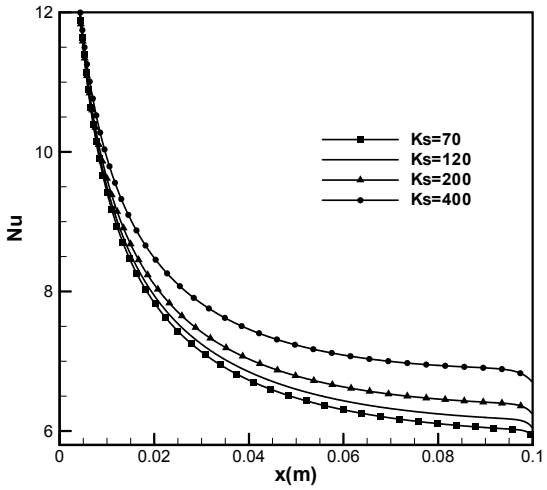

Fig. 11. Nusselt number distribution for different thermal conductivities of the solid region

Another way to consider the effect of axial conduction is to compare the interface wall temperature distribution along the channel for different height ratios. Fig. 10 shows the effect of increasing b from 10 to 100 on the interface wall temperature distribution for a 1% volume fraction Al_2O_3-EG/Water nanofluid flowing in the channel at Re_f=20 and q_w=10^5 W/m^2. Increasing the height ratio to values higher than critical one (b=67) will make axial conduction more dominant which causes the temperature distribution not to obey linear treatment along the channel. Another way to boost the effect of axial conduction is to change the kind of solid

region. Figure 11 illustrates the Nusselt number distribution along horizontal axis for the case of Re_f=250 and φ=0.02. Increasing the thermal conductivity of the solid region will enhance heat transfer to the fluid region. The fully developed Nusselt number Increases 11.5% by raising thermal conductivity from 120 w/m K to k_s=400 w/m K.

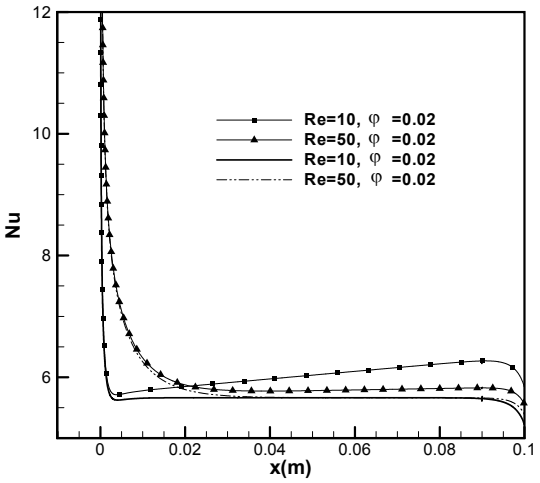

Fig. 12. The effect of variable properties on Nusselt number

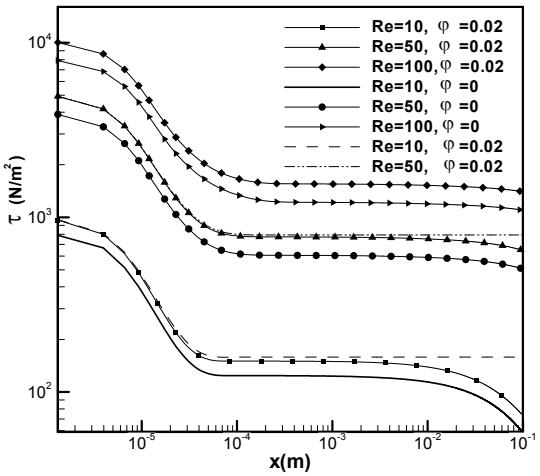

Fig. 13. The effect of variable properties and nanofluid concentration on shear stress of the lower wall

4.2 Variable Properties Effect

The effect of using variable properties with temperature is depicted in Fig. 12. A 2% volume fraction of nanofluid is flowing with Re_f=10 and 50 in a channel with b=7. The dashed lines in the figure show the Nusselt number distribution with constant thermal conductivity and dynamic viscosity along the channel. A slight difference between the two cases of constant properties and variable properties is seen at the end section in fully developed region which is a result of increasing the temperature along the channel, yielding augmentation in thermal conductivity.

The effect of different parameters on the shear stress in the lower wall of the fluid region is shown in Fig. 13. Dashed lines show the results obtained by constant properties assumption. The small reduction at the end parts of the channel in lower Reynolds numbers in comparison to constant properties cases is for the reduction of dynamic viscosity by temperature rise. This decline diminishes for higher Reynolds numbers as a result of small temperature changes. Adding nanoparticles will raise shear stress in the vicinity of the channel wall and it means more power is needed to pump the nanofluid. The effect of nanoparticles in shear stress is small in comparison with the effect on heat transfer characteristics but it should be noticed in heat exchanger design considerations.

Comparing the results of constant properties and variable properties reveals that considering variable properties, which is the more real one, will cause higher Nusselt numbers and lower shear stresses. Moreover, in the constant properties case, the fully developed Nusselt number is approximately the same for all of the Reynolds numbers, but this is not true for variable properties case.

5. CONCLUDING REMARKS

The effect of axial conduction and variable properties on the hydrodynamic and thermal characteristics of Al_2O_3-EG/Water nanofluid flowing in a two dimensional microchannel is studied in this paper. The overall results can be categorized as:

1- The fully developed Nusselt number will be augmented about 11.5% for φ=0.03 in comparison with pure mixture (φ=0).

2- Increasing volume fraction means more pumping power to make the fluid, flow in the channel.

3- As a result of considering conduction number, it was obtained that adding nanoparticles will weaken the axial conduction effect in microchannel.

4- Axial conduction effect causes a minimum in the Nusselt number distribution at the entrance length.

5- Using solid regions with higher thermal conductivities will enhance heat transfer by increasing Nusselt number and amplify axial conduction effect.

6- Considering variable properties will cause higher Nusselt numbers and lower shear stresses rather than constant properties.

REFERENCES

ASHRAE Handbook (2005). *Fundamentals*, American Society of Heating, Refrigerating and Air-Conditioning Engineers Inc., Atlanta, GA.

Bejan, A. and E. Sciubba (1992). The optimal spacing of parallel plates cooled by forced convection. *International Journal of Heat and Mass Transfer* 35, 3259-3264.

Bhattacharya, P., A.N. Samanta and S. Chakraborty (2009). Numerical study of conjugate heat transfer in rectangular microchannel heat sink with Al_2O_3/H_2O nanofluid. *Heat and Mass Transfer* 45,

1323–1333.

Brinkman, H. C. (1952). The viscosity of concentrated suspensions and solutions. *Journal of Chemical Physics* 20, 571–581.

Chiou, J.P. (1980). The advancement of compact heat exchanger theory considering the effects of longitudinal heat conduction and flow non-uniformity, *Symposium on Compact Heat Exchangers.* ASME HTD 10, 101-121.

Chon, C.H., K.D. Kihm, S.P. Lee and S.U.S. Choi (2005). Empirical correlation finding the role of temperature and particle size for nanofluid (Al_2O_3) thermal conductivity enhancement. *Applied Physics Letters* 87(15), 153107–153110.

Ferziger, J.H. and M. Peric (2002). *Computational Methods for Fluid Dynamics*, third ed., New York, USA: Springer.

Gamrat, G., M. Favre-Marinet and S. Le Person (2009). Modelling of roughness effects on heat transfer in thermally fully-developed laminar flows through microchannels. *International Journal of Thermal Sciences* 48, 2203-2214.

Hamilton, R.L. and K. Crosser (1962). Thermal conductivity of heterogeneous two- component systems. *Industrial and Engineering Chemistry Fundamentals* 1, 187- 191.

Hetsroni, G., A. Mosyak, E. Pogrebnyak, L.P. Yarin (2005). Heat transfer in micro-channels: Comparison of experiments with theory and numerical results. *International Journal of Heat and Mass Transfer* 48, 5580–5601.

Ho, C.J., L.C. Wei and Z.W. Li (2010). An experimental investigation of forced convective cooling performance of a microchannel heat sink with Al_2O_3/water nanofluid. *Applied Thermal Engineering* 30, 96–103.

Jang, S.P. and S.U.S. Choi (2006). Cooling performance of a microchannel heat sink with nanofluids. *Applied Thermal Engineering* 26, 2457–2463.

Jang, S.P. and S.U.S. Choi (2004). Role of Brownian motion in the enhanced thermal conductivity of nanofluids. *Applied Physics Letters* 84, 4316–4318.

Kandlikar, S.G. and W.J. Grande (2003). Evolution of microchannel flow passages – thermohydraulic performance and fabrication technology. *Heat Transfer Engineering* 24, 3–17.

Koo, J. and C. Kleinstreuer (2005). Laminar nanofluid flow in microheat-sinks. *International Journal of Heat and Mass Transfer* 48, 2652–2661.

Koo, J. and C. Kleinstreuer (2004). A new thermal conductivity model for nanofluids. *Journal of Nanoparticle Research* 6, 577–588.

Lee, P.S. and S.V. Garimella (2006). Thermally developing flow and heat transfer in rectangular microchannels of different aspect ratios. *International Journal of Heat and Mass Transfer* 49, 3060-3067.

Lelea, D. (2007). The conjugate heat transfer of the partially heated microchannel. *Heat and Mass Transfer* 44, 33–41.

Lelea, D., S. Nishio, K. Takano (2004). The experimental research on microtube heat transfer and fluid flow of distilled water. *International Journal of Heat and Mass Transfer* 47, 2817–2830.

Li, Z., Y.L. He, G.H. Tang and W.Q. Tao (2007). Experimental and numerical studies of liquid flow and heat transfer in microtubes, *International Journal of Heat and Mass Transfer* 50, 3447–3460.

Maiga, S.E.B., C.T. Nguyen, N. Galanis and G. Roy (2004). Heat transfer behavior of nanofluids in a uniformly heated tube. *Superlattices and Microstructures* 35, 543–557.

Masoumi, N., N. Sohrabi, A. Behzadmehr (2009). A new model for calculating the effective viscosity of nanofluids. Journal of Physics D: *Applied Physics* 42, 055501-055506.

Mintsa, H.A., G. Roy, C.T. Nguyen and D. Doucet (2009). New temperature dependent thermal conductivity data for water-based nanofluids. *International Journal of Thermal Sciences* 48, 363–371.

Morini, G. L. (2006). Scaling effects for liquid flows in microchannels. *Heat Transfer Engineering* 27(4), 64–73.

Nonino, C., S. Savino, S.D. Giudice, L. Mansutti (2009). Conjugate forced convection and heat conduction in circular microchannels. *International Journal of Heat and Fluid Flow* doi:10.1016/j.ijheatfluidflow.2009.03.009.

Pollard, A. and A.L.W. Siu (1982). The calculation of some laminar flows using various discretization schemes. *Computer Methods in Applied mechanics and Engineering* 35, 293-313.

Santra, A.K., S. Sen and N. Chakraborty (2009). Study of heat transfer due to laminar flow of copper–water nanofluid through two isothermally heated parallel plates. *International Journal of Thermal Sciences* 48, 391–400.

Tsai, T.H. and R. Chein (2007). Performance analysis of nanofluid-cooled microchannel heat sinks. *International Journal of Heat and Fluid Flow* 28, 1013–1026.

Tuckerman, D.B. and R.F.W. Pease (1981). High performance heat sink for VLSI. *IEEE Electron Device Letters* 2 126–129.

Vajjha, R. S., K.D. Das and P.K. Namburu (2010). Numerical study of fluid dynamic and heat transfer performance of Al_2O_3 and CuO nanofluids in the flat tubes of a radiator. *International Journal of Heat and Fluid Flow* 31, 613–621.

Vajjha, R.S. (2009). *Measurements of Thermophysical Properties of Nanofluids and Computation of Heat Transfer Characteristics*. M.S. thesis, Mech. Engineering Dept., University of Alaska Fairbanks, Fairbanks, AK.

Vajjha, R.S. and D.K. Das (2009). Measurement of thermal conductivity of three nanofluids and development of new correlations. *International Journal of Heat and Mass Transfer* 52, 4675–4682.

Wang, X., X. Xu, and S.U.S. Choi (1999). Thermal conductivity of nanoparticles–fluid mixture. *Journal of Thermophysics and Heat Transfer* 13(4), 474–480.

Xie, X.L., Z.J. Liu, Y.L. He and W.Q. Tao (2009). Numerical study of laminar heat transfer and pressure drop characteristics in a water-cooled minichannel heat sink. *Applied Thermal Engineering* 29, 64–74.

Xuan, Y. and and W. Roetzel (2000). Conceptions for heat transfer correlation of nanofluids. *International Journal of Heat and Mass Transfer* 43, 3701–3707.